Progress In Electromagnetics Research, PIER 101, 189–202, 2010

SIMULATION AND EXPERIMENTAL VERIFICATION OF W-BAND FINITE FREQUENCY SELECTIVE SURFACES ON INFINITE BACKGROUND WITH 3D FULL WAVE SOLVER NSPWMLFMA

S. Islam, J. Stiens, G. Poesen, and R. Vounckx

Laboratory for Micro- and Photonelectronics
Department of Electronics and Informatics
Vrije Universiteit Brussel
Pleinlaan 2, 1050 Brussels, Belgium

J. Peeters, I. Bogaert, and D. de Zutter

Department of Information Technology (INTEC)
Ghent University
Sint Pietersnieuwstraat 41, B-9000 Ghent, Belgium

W. de Raedt

IMEC
Department INTEGSYS
Kapeldreef 75, B-3001 Heverlee, Belgium

Abstract—We present the design, processing and testing of a W-band finite by infinite and a finite by finite Grounded Frequency Selective Surfaces (FSSs) on infinite background. The 3D full wave solver Nondirective Stable Plane Wave Multilevel Fast Multipole Algorithm (NSPWMLFMA) is used to simulate the FSSs. As NSPWMLFMA solver improves the complexity matrix-vector product in an iterative solver from $\mathrm{O}(N^2)$ to $\mathrm{O}(N \log N)$ which enables the solver to simulate finite arrays with faster execution time and manageable memory requirements. The simulation results were verified by comparing them with the experimental results. The comparisons demonstrate the accuracy of the NSPWMLFMA solver. We fabricated the corresponding FSS arrays on quartz substrate with photolithographic etching techniques and characterized the vector S-parameters with a free space Millimeter Wave Vector Network Analyzer (MVNA).

Corresponding author: S. Islam (sislam@etro.vub.ac.be).

1. INTRODUCTION

Highly coherent millimetre wave illumination leads to poor image quality, disturbed by noise sources in active imaging [1]. As such the destruction of the coherence level is a prerequisite to obtain sufficient image quality [2]. The mm-wave coherence controllable diffuser can be designed with complex grounded FSS array where the elementary blocks are finite size FSS arrays. For the design of such practical diffuser system it is very important to know the characteristic of finite extent FSS arrays [2, 3].

The FSSs are passive electromagnetic filters formed by periodic thin conducting elements on a dielectric substrate or periodic aperture elements in a conducting sheet [4]. Typically the analyses of FSSs and other planar periodic structures are carried out under the assumption that they are infinite in extent, even though the dimensions of practical FSS structures are necessarily finite. A number of methods, e.g., mode matching, the moment method [5–9], the spectral-Galerkin approach [10], and certain approximate methods, are available for analyzing infinite periodic structures. The problem of scattering from infinite (i.e., doubly-periodic) FSSs has been researched extensively for many years by using the Floquet theorem that reduces the computation domain to a single unit cell, and thus reduces the problem to a manageable one. However, this cannot be applied for the moderate size finite FSS array problem, which is much more difficult to handle and, to our knowledge, has not been treated in a general way without any approximation. Simulations based on the generally applied infinite-array approach do not describe boundary effects and simulation of the finite array method is computationally too expensive.

There are several method used to simulate finite FSS array. Interactive method deals with a relatively small-size FSS, which is treated via the Spectral-Galerkin method that accounts for all of the interactions between the elements in a rigorous way. However, this method is not well-suited for larger surfaces as it places a heavy burden on the CPU memory and time requirements; both of which become very rapidly unmanageably large with increasing array size. Truncation methods, based on the plane wave spectral (PWS) decomposition approach are also used to simulate finite FSS arrays. This approach enables to treat the finite FSS problem as though it were doubly periodic and infinite. In this method a finite FSS array is approximated by an infinite one, which is locally illuminated. Though the truncation or approximation method is very general-purpose, can handle the problem of a finite FSS illuminated by an arbitrary excitation, highly efficient for large FSS geometries,

memory requirement is relatively low but the method is also prone of problems. In some instances, the physical size of the array and the frequency of operation are such that the infinite periodic assumption introduces negligible errors, particularly when the surface is used near resonance. However, it has been demonstrated [6–8] that, in many other situations, the truncation effect plays a rather significant role in altering the current distribution, as they introduce higher cross-polarized components, excite surface waves and cause extraneous radiation. Thus the edge effect must be carefully accounted for in order to accurately predict the scattering characteristics of a finite FSS, particularly at out of band frequencies [9].

The finite array simulations should meet a number of criteria: they should be fast executable, they should show boundary effects and effects of mutual coupling, and they should determine the antenna performance parameters accurately [11, 12]. All attempts at incorporating the finite nature of the array have been hampered by the limitation of computer memory and execution timing. This is because, unlike the periodic problem where it is sufficient to deal with the unknown currents over a single unit cell, it now becomes necessary to treat the entire individual currents on each cell as separate unknowns. Full-wave simulation of finite FSS, based on the Maxwell equations, is gaining importance now that technology has reached a point where many of the quasi-static or high-frequency approximations are no longer sufficiently accurate. A major drawback of the so-called exact methods is their greed for resources, namely CPU-time and computer memory. Industry puts a limit to both, inspiring the quest for ever more powerful methods. To overcome the CUP timing and memory requirement the 3D full wave solver Nondirective Stable Plane Wave Multilevel Fast Multipole Algorithm (NSPWMLFMA) is used in this work [13–15]. By employing NSPWMLFMA, the complexity is reduced from $\mathrm{O}(N^2)$ to the order of $\mathrm{O}(N \log N)$ at all frequencies [15, 16]. In addition to this, the entire implementation (both the setup and the solution of the iterative process), has been parallelized using an asynchronous algorithm, such that all simulations can be solved efficiently on a cluster of computers.

In this study, we will compare the simulation results of finite FSS on infinite background (e.g., Fig. 1) obtained with NSPWMLFMA 3D solver to experimental results. On the basis of experimental and simulation results, we wanted to find characteristics that describe the (qualitative) behavior of such finite FSS arrays. In particular, we wanted to find characteristics which eventually will give the opportunity to check the finiteness behavior of the array.

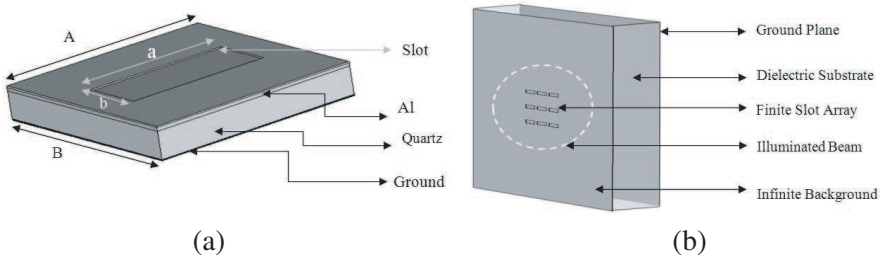

Figure 1. Finite grounded FSS array: (a) unit cell configuration and (b) finite grounded FSS array on infinite background. The antenna size is smaller (i.e., finite) whereas the background is very large (i.e., infinite) in compare to the illumination.

This paper is organized as follows: Section 2 describes the definition of test cases of finite × infinite and finite × finite FSS arrays. Section 3 presents the fabrication process of FSS arrays. In Section 4, the Nondirective Stable Plane Wave Multilevel Fast Multipole Algorithm (NSPWMLFMA) solver has been reported. Section 5 presents the experimental setup of MVNA for antenna measurement in W-band. In Section 6, the simulation and experimental results of finite arrays are presented. In Section 7, a discussion on simulation and experimental results has been made. Finally in Section 8, some conclusions are drawn on the basis of this comparison results.

2. DEFINATION OF TEST CASES

The structures under consideration are a 4 × 4 cells finite by finite and a 4 × 22 finite by infinite grounded slot FSS arrays as shown in Figs. 2(a) and (b). The millimeter wave illumination beam spot size is limited due to the laser like coherence characteristics of millimeter wave sources. If the antenna size smaller than the illumination beam spot size we can call the antenna finite compared to the illumination. For the sumilation case the 4×4 cells array is not smaller than the 4×12 array, because the finite ground plane is taken into account. Hence, in absolute size, they are equally large (despite the one having fewer slots than the other). As a consequence, few commercial solvers are available for full wave simulation of such finite array without approximation of the edge effects.

The periodicity of the array, i.e., unit cell dimensions are set to $A = B = 1250\,\mu\text{m}$ and the layout of the structure is shown in Fig. 1(a). The slots are etched in Aluminum backed by metal backed quartz of dielectric constant 3.78 and loss tangent 0.0001 as shown in Fig. 2. The

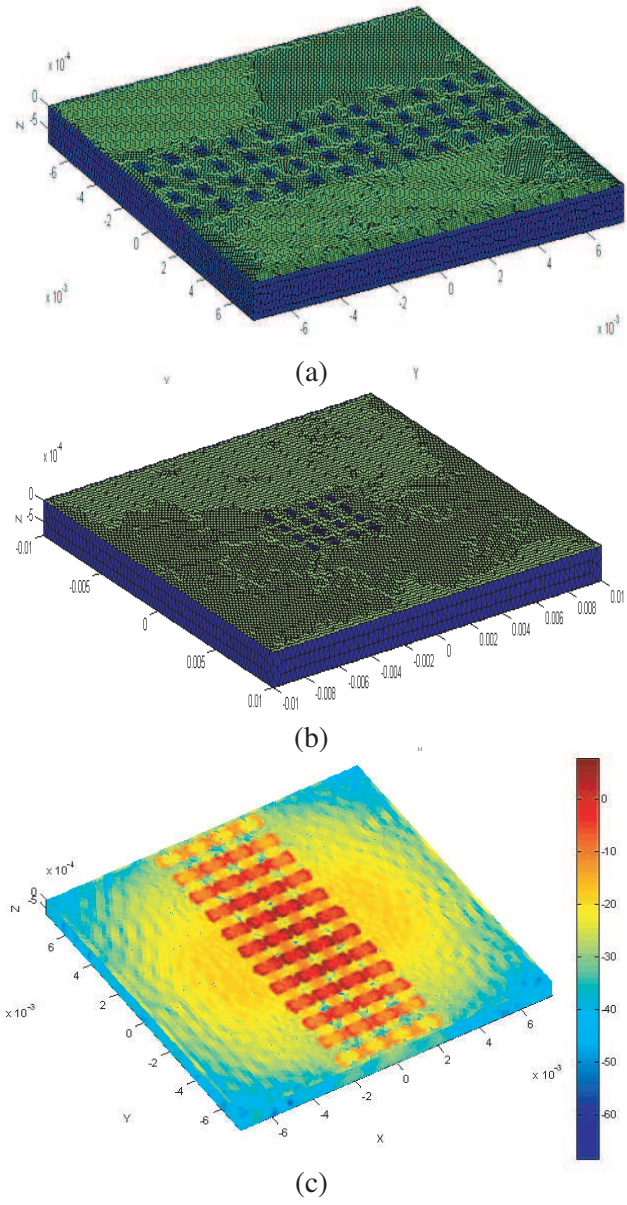

Figure 2. Finite grounded FSS array simulation with NSPWMLFMA solver: (a) meshing of finite × infinite array, (b) meshing of finite × finite array and (c) current distribution of the finite × infinite FSS array.

substrate thickness is 800 μm and the Aluminum thickness is 1.5 μm. The meshing used in the 3D NSPWMLFMA solver for the 4 × 22 cells finite by infinite and 4 × 4 cell finite by finite grounded FSS arrays simulation are shown in Figs. 2(a) and (b) respectively. Note that the finite thickness of Aluminum was not included in the meshing. At the time, this is not yet possible with 3D NSPWMLFMA solver and we used an infinitely thin PEC plate. The illumination beam width is approximately equal to the of 8 × 8 cells size on the array. The current distribution of the finite × infinite FSS array is shown in Fig. 2(c).

2.1. Finite × Infinite Array

Finite × infinite arrays is also called H-plane finite array. Instead of modeling a rectangular uniform slot array as being finite in length and width direction, the array is modeled as being finite in the H plane direction and infinite in the E plane direction as shown in Fig. 2(a). The array solution is based on the assumption of infinite array plus addition of edge effects. The infinite background size is $8.6\lambda \times 8.6\lambda$ i.e., with 1.3 cm × 1.3 cm physical dimensions where total number of FSS unit cells are 88 (e.g., 4 × 22 slots).

2.2. Finite × Finite Array

Finite × finite array is both E-plane and H-plane finite array. In this case, the modeling is with a rectangular uniform array as being finite both in the E plane and in the H plane directions as shown in Fig. 2(b). The array size is 0.5 cm × 0.5 cm and the background size is 2.5 cm × 2.5 cm. The finite × finite array is with 16 cells (e.g., 4 × 4 slots) and the background size is same as in the case of finite × infinite array.

3. FABRICATION

The FSS arrays were fabricated on a grounded quartz substrate. The basic unit cell of the array is shown in Fig. 1(a). The slots (width: 400 μm, length: 786 μm) are etched in Aluminum on the quartz substrate (relative permittivity: 3.78, loss tangent: 0.0001, thickness: 800 μm). Slot length (786 μm) is chosen so that the resonant frequency is approximately at 85.5 GHz. The maximum number of allowable defect per square inch was 2. The minimum feature size (i.e., critical dimension) we measured and controlled in the fabrication process was 5.0 μm.

4. SIMULATION WITH 3D NSPWMLFMA SOLVER

Cassandra is a full-wave three-dimensional solver. Solution is accelerated through the use of advanced ML-FMA methods, stable at all frequencies. It supports dielectric and perfectly electric conducting, which can be embedded and touch each other. Using an asynchronous parallel framework (Nexus), it is perfectly suitable for simulation of scattering problems at very large and complicated geometries [17, 18]. Cassandra is based upon surface integral equations and therefore requires a triangular mesh of the geometry. A number of incoming (external) fields are supported, including plane wave, and as well as Gaussian beam. The simulation is done by using Boundary Integral Equations (BIE) and solves them using a Method of Moments (MoM). MoM has $O(N^2)$ complexity, which makes large simulations very hard. However, we accelerate the MoM by applying Fast Multipole Methods (MoM). The current algorithm is a hybrid that covers both low frequencies (using NSPWMLFMA) and high frequencies (MLFMA) with an elegant transition between them. The broadband FMM algorithm is based on two distinctive FMM methods. In the FMM tree, interactions between boxes that are larger than approximately 0.25λ are treated with the MLFMA. However, the MLFMA becomes unstable if any of the boxes would be smaller than this. As a consequence, levels where the boxes are smaller than 0.25λ are treated with the NSPWMLFMA, which essentially stabilizes the MLFMA but is slightly more expensive in terms of computation requirements (which explain why it can't be used at high frequencies as well). Between the levels where treatment with the NSPWMLFMA changes to using the MLFMA, a special interpolator is used to do the transition between the two methods. Because the NSPWMLFMA is simply an extension of the MLFMA (based on a normalization of the terms in its plane wave decomposition), this interpolation is particularly elegant, which is part of the NSPWMLFMA's appeal. Employing these techniques, the complexity is reduced to $O(N \log N)$ at all frequencies which gives the facilities to simulate the moderate and large size finite arrays without any approximation [19]. In addition to this, we have parallelized the entire implementation (both the setup and the solution of the iterative process), using an asynchronous algorithm, such that all simulations can be solved efficiently on a cluster of computers [19].

5. EXPERIMENTAL SETUP

The W-band (75–110 GHz) measurement setup of free space Millimeter Wave Vector Network Analyzer (MVNA) is shown in Fig. 3(a). The

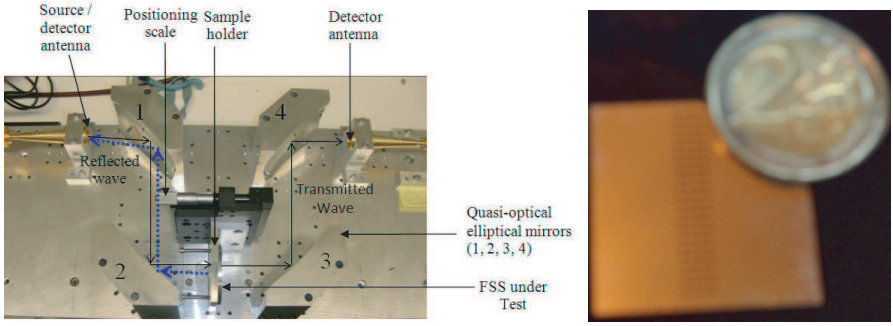

Figure 3. W-band MVNA setup for FSS measurement: (a) photo of MVNA with schematics of the reflected and transmitted beams and (b) photo of the manufactured and measured 4 × 22 cells finite by infinite FSS array.

MVNA is calibrated with the open short calibration method for the FSS measurement. The baseline calibration is done by first making a calibration measurement without any DUT (Device under Test) while still recording the results. A suitable reference for the reflections of the DUT is obtained by making the calibration measurement with a short circuit as a calibration load. This follows from the fact that a short circuit in the test port of MVNA reflects quite precisely the entire test signal. Ideally the transmission and reflection responses would be directly related to the scattering parameters S_{21} and S_{11} of the DUT respectively. Then later the measurement results with the DUT are divided by the recorded results of the calibration measurement. The final outcome of this procedure is that the MVNA system can display both amplitude and phase of the DUT. After the calibrating the MVNA the antenna under test is placed between the antenna holder and the fixing ring as shown in Fig. 3(a). The reflected beam from the antenna is indicated by dotted line. A directional coupler is connected with the source antenna so that the same antenna can be used as the detector antenna in reflection measurements.

6. RESULTS

The physical slot elements areas of the finite × infinite and finite × finite are 5 mm × 27.5 mm and 5 mm × 5 mm respectively on 2.5 cm × 2.5 cm metalic backgrounds. The illumination beam spot size of the Millimeter Wave Vector Network Analyzer (MVNA) is approximately

1.5 cm. Hence the arrays can be treated as finite by infinite and finite by finite arrays. A photo of the manufactured and measured 4×22 cells finite by infinite FSS array is shown in Fig. 3(b). The measurement and simulation results of the finite $\times$ infinite and finite $\times$ finite arrays are presented separately below. All the measurements are done with the quasi optical free space MVNA as shown in Fig. 3(a).

6.1. Finite $\times$ Infinite Array

The first array we consider is a finite by infinite array of 4×22 cells. Fig. 4 shows the simulation and measurement comparison which demonstrates good agreement both for the S_{11} amplitudes and phases. he measured S_{11} amplitude shows larger attenuation at resonance and wider bandwidth compared to the simulation results. Fig. 4 shows that the measured centre frequency of the finite $\times$ infinite FSS array is at 85.59 GHz and the bandwidth is 3.35 GHz (e.g., -3 dB points), while in the simulation center frequency of the array is 85.5 GHz and the -3 dB band width is 3.2 GHz. So the resonant frequency shifts 0.09 GHz and bandwidth enlargement in the measurement result is 0.15 GHz. The measured attenuation at resonant is -15.88 dB compared to -8.733 dB simulation value. When the reflection amplitudes decreases from -3 dB to -15.88 dB the frequency decreases from 83.83 GHz to 58.59 GHz. In the stop band, there is an attenuation of -15.88 dB. The minimum measurement phase value is 129.38 degree at 85 GHz compared to the simulation value of 116.3 degree. The maximum phase value we measured is 232.85 degree at 86 GHz whereas the simulation value is 212.84 degree.

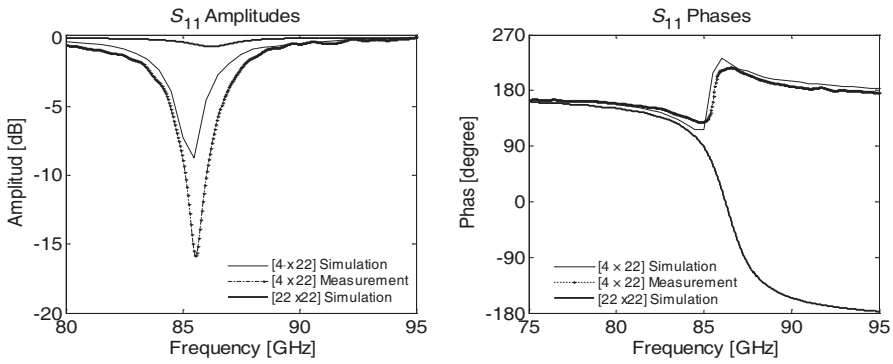

Figure 4. Simulation and measurement comparison of 4×22 cells finite $\times$ infinite array on infinite metallic background: (a) Amplitudes and (b) phases.

The measured phase curves show a slight mismatch compared to the simulation but both of them show the antenna/metal weighted balancing reflection. Simulation phase curve shows larger phase variation than the measurement which indicates that the antenna/metal ratio is slightly higher in measurement case compared to the simulation. We have shown in the experimental characterization of finite × infinite array case that the reflection amplitudes and phase of finite × infinite array is the balancing weighted reflection from the effective antenna/metal area. The results can be interpreted as follows: the shifting of resonant frequency of the finite array is a function of the number of slots in the tangential magnetic field (i.e., H_t) direction and the effective illuminated background area. For the sake of comparison we also added the simulation amplitude and phase curves of infinite slot FSS array when an ideal plane wave is incident on it. Fig. 4 clearly shows the difference of infinite and finite array simulations.

6.2. Finite × Finite Array

Figure 5 shows the simulation and measurement comparison of 4 × 4 cells finite array of Fig. 2(b). The measurement in this case also shows higher attenuation and wider bandwidth compared to the simulation results. This is due to the mismatch of effective antenna/metal ratio of both the simulation and the measurement structures. We also observe the resonant frequency shifting effect. Due to the resonance shifting a shift of phase is measured. Other than these both the simulation S_{11} amplitude and phase curves fit well with those of the measured curves. The Fig. 5 shows that the measured centre

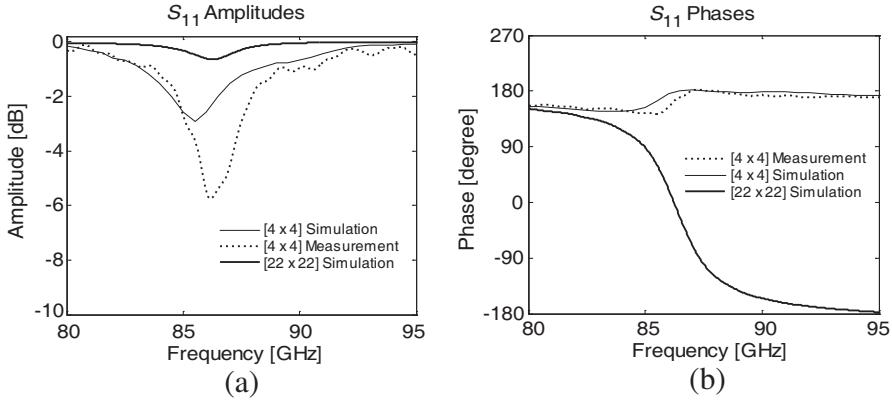

Figure 5. Simulation and measurement comparison of 4 × 4 cells finite × finite array on infinite metallic background: (a) Amplitudes and (b) phases.

frequency of the finite × finite FSS is 86.15 GHz and −3 dB bandwidth is 2.29 GHz, while the simulation center frequency of the array is 85.5 GHz, and the reflection amplitude at resonance is −2.91 dB. So the simulation bandwidth of the finite by finite array is full W-band. The measured attenuation at resonant is −5.75 dB in compare to −2.91 dB of simulation value. When the reflection loss decreases from −3 dB to −5.75 dB the frequency increases from 85.16 GHz to 86.15 GHz. In the stop band, there is an attenuation of −5.75 dB. The minimum measured phase value is 146° degree at 85.55 GHz in compare to the simulation value of 149° degree at 84 GHz. The maximum phase value we measured is 181° degree at 87.23 GHz whereas the simulation value is 182.46 degree. For the comparison purpose it is interesting to add the simulation amplitude and phase curves of infinite slot FSS array (i.e., 22 × 22 cells array) with ideal plane wave excitation. Fig. 5 represents the difference of finite by finite array characterization (e.g., simulation measurement comparison) and the behavior of its infinite extent.

7. DISCUSSION ON COMPARISON RESULTS

Except classical measurement errors (e.g., drift error, random errors, systematic errors, error due to multi reflections between the source port and the antenna under measurement, errors due to limited directivity of the directional device etc.), there are several considerations which we need to count as the sources of measurement errors. The main mismatches are illumination beam size variation, beam type mismatch in simulation and measurement and the weighted FSS array/metallic background area sensitivity.

(1) It is difficult to get a proper match between the beam size considered in the simulation (e.g., 1.59 cm) and the beam sizes used in the measurement. In the simulation the illumination beam size was considered constant though the MVNA beam width varies with the change of frequency. In the W band (e.g., 75 GHz to 110 GHz) the illumination beam diameter is in the range of 1.59 cm $\sim$ 1.1 cm. As the measurement result of finite array is very much sensitive to antenna array/effective background area, consequently the measured result will somehow differ from the simulation.

(2) In the finite FSS arrays simulation instead of finite thick of Aluminum infinitely thin PEC plate was included as it is not yet possible with 3D NSPWMLFMA solver to simulate finite thick of Aluminum. Moreover, a constant illumination is not realistic with ideal shape used in the simulation. Hence, the analysis method introduces some approximations that also cannot be reproduced in the measure of the manufactured antennas.

(3) The FSS response is the weighted balance of the effective FSS area and the metallic background as a consequence probability to introduce errors in the measurement is high.

(4) Type of illumination beam mismatch is another source of errors. The simulation was carried out with the Gaussian beam approximated as plane waves. In the measurement system the illumination of the MVNA source horn antenna radiation is consider as plane wave. So the probability of accurate beam type matching is obviously not negligible.

As we see from the above measurement and simulation comparisons (e.g., Fig. 4 and Fig. 5) that the larger difference in the measured S_{11} amplitudes in compared to the simulation results. In both the finite × infinite and finite × finite the measured S_{11} amplitudes shows higher attenuation in compare to the simulation amplitudes. To verify the above discussion we will consider the measurement and simulation comparison of results of finite × infinite array again. This time we will compare the simulation result with three measurement results as shown in Fig. 6 below. The three measurements were taken on the antenna surface where meas. 1 is at the centre of the FSS array and the other two (meas. 2 and meas. 3) are off centre measurement.

Now we see that that the simulation and the measured S_{11} amplitudes are almost equal, though there is a frequency shift in case of the off centre measurements. It is because now the antenna/metal background ratio is different than the case of meas. 1 (e.g., at centre measurement). Hence the point (1) in the above discussion is logical.

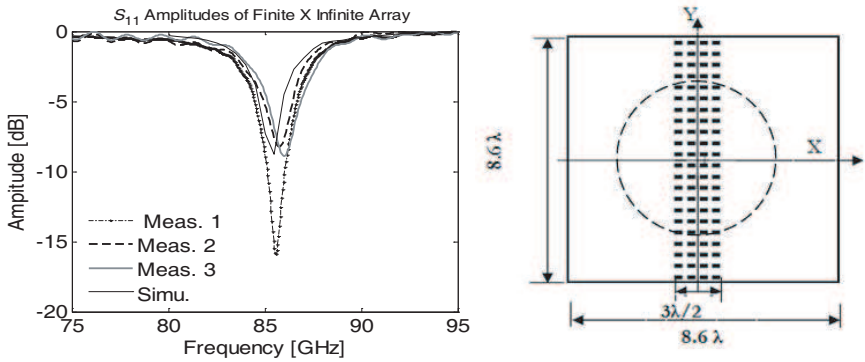

Figure 6. (a) Simulation and measurement comparison of 4 × 22 cells finite × infinite FSS array and (b) illumination beam positions: 'Meas.1' at the antenna centre, 'meas.2' and 'meas.3' are off centre measurement positions.

8. CONCLUSION

This study aimed at comparing the simulation and measurement results of finite and semi-infinite FSS arrays compared to the illumination beam size to investigate the effects of finite array and infinite beam size on the reflection characteristics of FSSs. As basic elements we chose the grounded FSS arrays. The simulation results obtained from 3D full wave solver NSPWMLFMA agree pretty well with the experimental results. We have presented a clear view in the order of magnitudes change of amplitudes and phases when the dimensions of the arrays are finite compared to the illumination beam size. The full wave simulation results show well agreement with the experimental results.

ACKNOWLEDGMENT

This work was partially funded by the Vrije Universiteit Brussel (VUB-OZR), and the Flemish Institute for the encouragement of innovation in science and technology (IWT-SBO 231.011114).

REFERENCES

1. Koers, G., "Noise suppression in active millimeter wave imaging systems," Ph.D. dissertation, Universiteit Brussel, July 2006.
2. Islam, S., J. Stiens, G. Poesen, I. Jäger, and R. Vounckx, "Passive frequency selective surface array as a diffuser for destroying millimeter wave coherence," *Active and Passive Electronic Components*, Vol. 2008, 2008.
3. Islam, S., J. Stiens, G. Poesen, I. Jäger, and R. Vounckx, "Implementation of dynamic hadamard diffuser as a frequency selective surface for W-band active millimeter wave imaging," *Microwave and Optical Technology Letters*, Vol. 51, No. 6, 1440–1444, June 2009.
4. Kastner, R. and R. Mittra, "Iterative analysis of finite-sized planar frequency selective surfaces with rectangular patches or perforations," *IEEE Trans. Antennas Propagat.*, Vol. 35, No. 4, 372–378, 1987.
5. Chen, C. C., "Transmission through a conducting screen perforated periodically with apertures," *IEEE Trans. Microwave Theory Tech.*, Vol. 18, No. 9, 627–632, 1970.
6. Chen, C. C., "Diffraction of electromagnetic waves by a conducting screen perforated with circular holes," *IEEE Trans. Microwave Theory Tech.*, Vol. 19, No. 5, 475–481, 1971.

7. Lee, S. W., "Scattering by dielectric-loaded screen," *IEEE Trans. Antennas Propagat.*, Vol. 19, No. 5, 656–665, 1971.
8. Montgomery, J. P., "Scattering by an infinite periodic array of thin conductors on a dielectric sheet," *IEEE Trans. Antennas Propagat.,* Vol. 23, No. 1, 70–75, 1975.
9. Agrawal, V. D. and W. A. Imbriale, "Design of a dichroic *Cassegrain* subreflector," *IEEE Trans. Antennas Propagat.*, Vol. 27, No. 4, 466–473, 1979.
10. Tsao, C. H. and R. Mittra, "Spectral domain analysis of frequency selective surfaces comprised of periodic arrays of cross dipoles and Jerusalem cross," *IEEE Trans. Antennas Propagat.*, Vol. 32, No. 5, 478–486, 1984.
11. Munk, B. A., "Scattering from surface waves on finite FSS," *IEEE Trans. Antennas Propagat.*, Vol. 49, No. 12, 2001.
12. Bekers, D., "Finite antenna arrays: An eigencurrent approach," Ph.D. dissertation, Technische Universiteit Eindhoven, 2004.
13. Fostier, J. and F. Olyslager, "Full-wave electromagnetic scattering at extremely large 2D objects," *IET Electronics Letters*, Vol. 45, No. 5, 245–246, 2009.
14. Van Den Bulcke, S. and A. Franchois, "A full-wave 2.5D volume integral equation solver for 3D millimeter-wave scattering by large inhomogeneous 2D objects," *IEEE Trans. Antennas Propagat.*, Vol. 75, No. 2, 535–545, Feb. 2009.
15. Song, M., T. Weng, and W. C. Chew, "Multilevel fast multipole algorithm for elastic wave scattering by large three-dimensional objects," *Journal of Computational Physics*, Vol. 228, No. 3, 921–932, 2009.
16. De Zaeytijd, J., A. Franchois, and J. M. Geffrin, "A new value picking regularization strategy — Application to the 3D electromagnetic inverse scattering problem," *IEEE Trans. Antennas Propagat.*, Vol. 57, No. 4, 1133–1149, 2009.
17. Chew, W. C., J. Jin, E. Michielssen, and J. Song, *Fast and Efficient Algorithms in Computational Electromagnetics*, Artech House, Boston, 2001.
18. Bogaert, I., J. Peeters, and F. Olyslager, "A nondirective plane wave MLFMA stable at low frequencies," *IEEE Trans. Antennas Propagat.*, Vol. 56, 3752–3767, 2008.
19. Wallèn, H. and J. Sarvas, "Translation procedures for broadband MLFMA," *Progress In Electromagnetic Research*, PIER 55, 47–78, 2005.